DEVELOPMENT OF AMV HEIGHT ASSIGNMENT DIRECTLY LINKED TO FEATURE TRACKING AT JMA

Ryo Oyama [1], Régis Borde [2], Johannes Schmetz [2] and Toshiyuki Kurino [1]

1 Meteorological Satellite Center of Japan Meteorological Agency
3-235 Nakakiyoto, Kiyose, Tokyo 204-0012, Japan
2 EUMETSAT, Am Kavalleriesand 31, D-64295 Darmstadt, Germany

ABSTRACT

The Height Assignment (HA) is one of the most important sources of errors in the operational Atmospheric Motion Vectors (AMVs) extraction schemes. The main difficulty in HA is to estimate the AMV height using individual image pixels that really lead to the feature tracking process. Following recent study which had been conducted by Japan Meteorological Agency (JMA) and EUMETSAT, the Meteorological Satellite Center (MSC) of JMA plans to develop a HA scheme that includes information on the individual-pixel contribution rate to the tracking process by cross-correlation matching. In this study, a new prototype scheme which is based on the weighted mean of IR1 (10.8 micro-meter) pixel radiances by the individual-pixel contribution rate to tracking process is tested. In the research comparing the heights of IR AMVs estimated by the new scheme to the ones obtained by the current JMA's HA scheme, the application of the new scheme reduces the fast-wind-speed bias in the middle troposphere, which is presently observed in the current JMA's AMVs.

1 INTRODUCTION

Atmospheric Motion Vectors (AMVs) is one of the most important wind products derived from satellite images because it is used in Numerical Weather Prediction (NWP) models. In particular, height assignment (HA) is one of the main important sources of error in AMVs extraction schemes. Particularly, the selection of pixels for computing AMV height is a very difficult problem.

In general, the height of cirrus cloud, which is good tracking-tracer, is replaced by the uppermost (coldest) cloud height within template image used for the feature-tracking. At JMA, the AMVs are assigned to the most frequent cloud height derived from height-histogram accumulated by 50-hPa intervals (Oyama and Shimoji, 2008). EUMETSAT uses the coldest peak of the cloud top height histogram included in the Cloud Analysis (CLA) product (ASD internal EUMETSAT document). NOAA / NESDIS uses a fixed threshold of 25 % coldest pixels for GOES instruments (Daniels, 2002). However, the current pixel selections without any information on feature-tracking could lead to HA errors because template image used for feature-tracking usually contains various clouds with different heights and movements (Borde, 2006).

To resolve the problem on the pixel selection for HA, Büche et al. (2006) considered individual pixel contribution to feature-tracking under cross-correlation matching, and applied it to the height computation of clear-sky-region WV AMVs. In that study, they indicated some positive impact on the accuracy of the AMVs data. Following this work, Borde and Oyama (2008) investigated the possibility to improve the AMV HA in infrared window channels, applying this information to METEOSAT-8 IR images.

In this study, the contribution rate to feature-tracking is applied to HA of upper and middle tropospheric IR AMVs using MTSAT-1R images and JMA's AMV processing system. The tested HA scheme was developed at JMA in collaboration with EUMETSAT. In section 2, contribution-rate to feature tracking under cross-correlation matching is introduced. In section 3, the characteristics of test AMVs are described under the comparison to the current JMA's current AMVs or other experimentally generated AMVs.

2 CONTRIBUTION RATE TO TRACKING IN CROSS-CORRELATION MATCHING

The definition of individual pixel contribution rate to feature-tracking (CCij) using cross-correlation matching is shown by Eq.1 (Büche et al. (2006)).

$$cc(m,n) = \frac{1}{MN}\sum_{i=1}^{M}\sum_{j=1}^{N}\frac{A_{i+m,j+n}-A_{mean}(m,n)}{\sigma_A(m,n)}\frac{B_{ij}-B_{mean}}{\sigma_B} = \sum_{i,j}^{M,N} cc_{ij} \quad \text{(Eq.1)}$$

CC (m,n): cross-correlation at the location best corresponding to the target in the second searching image
M, N: template image size (=32 at JMA)
A_{ij}, B_{ij}: each-pixel (i, j) radiance of target image and searched area image on the second searching image
A_{mean}, B_{mean}: averages of A and B, CCij : each pixel (i, j) contribution rate to feature tracking of each pixel (i, j)

CCij are computed by using the radiances in the first image and searched image in the second searching image of MTSAT-1R. They represent the individual contribution of each pixel within template image to the cross-correlation coefficient. Borde and Oyama (2008) indicate the general characteristics of CCij and illustrate the potential benefits of using such information in HA process, that is, (1) CCij of colder cloud pixel tends to be larger, and (2) Use of CCij allows removing cloudy pixel radiances that have large time variability between the successive images for tracking.

3 APPLICATION OF CONTRIBUTION RATE TO HEIGHT ASSIGNMENT

3.1 METHODOLOGY

The tracking of a cirrus cloud is illustrated in Figure 1(a) and (b), which represent the distributions of IR (10.8 micro-meter) Equivalent Black Body Temperature (EBBT) for the template image and searched-area image segment within the searching image, respectively. Figure 1 (c) and (d) are IR radiances which correspond to (a) and (b), respectively. Figure 1 (e) shows CCij for the template image, which are computed from radiance data in Figure1 (c) and (d). In this study, representative cloudy radiance which is computed by weighting the pixel radiances by their individual CCij (hereafter, the radiance is referred as L1) is used to compute heights for upper and middle height-level IR AMVs. L1 is defined as Eq. 2.

$$L1 \equiv \frac{1}{\sum_{i,j}^{pixels\_in\_Area1} CC_{ij}} \sum_{i,j}^{pixels\_in\_Area1} L_{i,j}^{cor} \times CC_{ij} \qquad \textbf{(Eq.2)}$$

Here, L^{cor}_{ij} is IR radiance of each pixel (i, j) corrected by using H2O-IRW intercept method (Nieman et al., 1993; Schmetz et al., 1993). In the computation of L1, the appropriate pixel selection from the template image for HA (i.e., how to decide *Area1* in Eq.2) is the main interesting problem.

In the following, Figure 1 (f) shows the scatter plots of CCij against IR radiance for the template image. L1 is calculated by using only the pixels that have a positive CCij. That is, pixels have CCij less than 0 (inside yellow region in Figure 2 (f)) or corresponding to the background, i.e., surface and so on (inside grey region in Figure 2 (f)) are excluded of the calculation. Finally, L1 is converted to an AMV height by using MTSAT-1R's conversion table between IR channel radiance and temperature, and vertical profile data of JMA's NWP (60km Global Spectral Model (GSM)) first-guess.

In a preliminary investigation, L1 was applied to all cloud targets for upper and height-level AMVs extracted by JMA's target selection scheme, where cloud pixels above 500 hPa height-level make up more than 5 % of all the pixels within template image. As the results, it was found that L1 could give relevant AMV heights in many cases. However, in some cases, for example AMVs in cloud areas below stable-layer at middle troposphere over the sea, the heights computed by L1 tend to be higher than the best-fit-levels against sonde observation and JMA's NWP. In fact, it is well known that the decision of the best AMV heights depends on the cloud types. Generally, the upper and middle height level AMVs should be assigned to cloud top height, in contrast, lower-height-level AMVs for cumulus to the cloud-base heights (Le Marshall et al., 1993). To apply L1 to cloud targets except for lower-height-level cloud targets, the cloud-type judge using by cross-correlation value between the template images of IR and WV EBBT is introduced in this study.

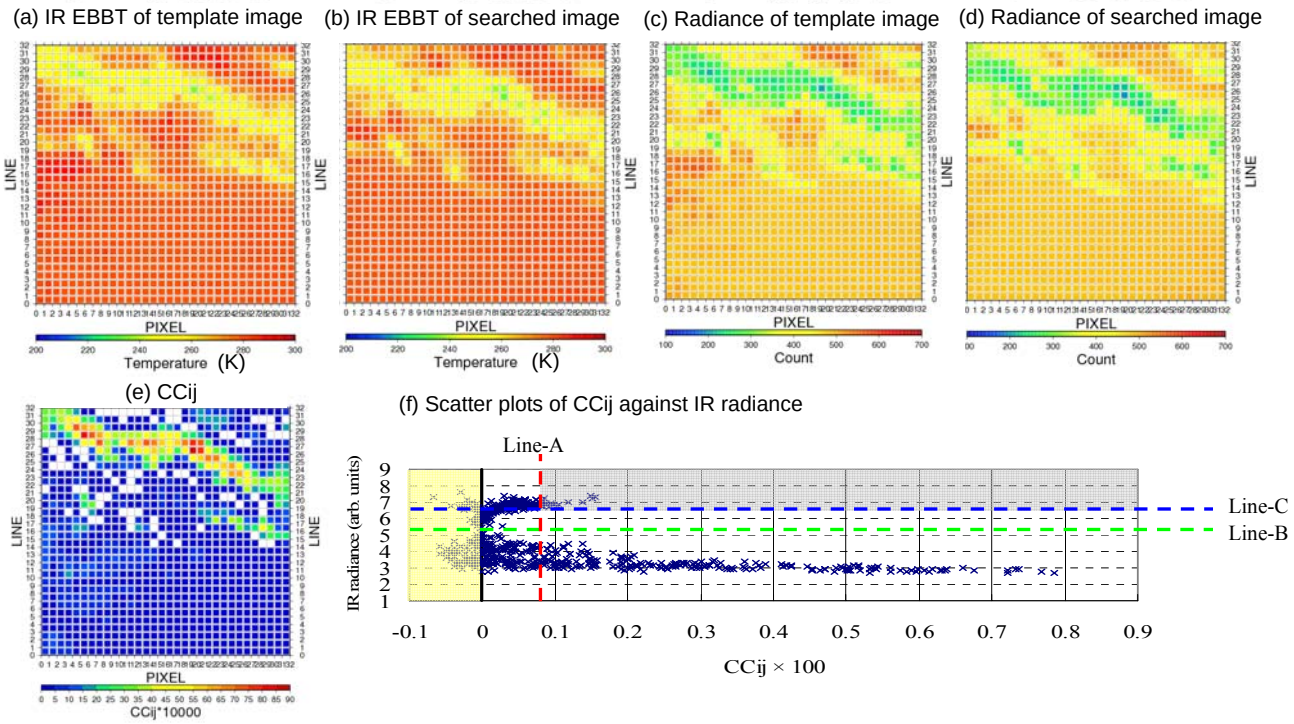

***Figure 1*: An example of AMV's template image at (35S,131E) at 12UTC on 10 March 2007.**
(a) The distribution of IR EBBT for template image
(b) Same as (a), but for searched image segment on the searching area
(c) The distribution of IR radiances (count unit) corresponding to Figure (a)
(d) The distribution of IR radiances (count unit) corresponding to Figure (b)
(e) CCij computed from IR radiances in Figure (c) and (d).
(f) Scatter plots of CCij against IR radiance (not corrected by H2O-IRW intercept method)
Pixels inside grey region (corresponding to background) and yellow region (pixels with negative CCij) in Figure (f) are not used in the computation of L1 by Eq.2.
Red line (Line-A): average cross-correlation per one pixel (=cross-correlation / (template size)^2)
Green line (Line-B): average of IR radiance
Blue line (Line-C): intersection of Line-A and quadratic curve of pixel distribution

Figure 2 shows (a) IR EBBT image, (b) wind vectors of AMVs, and (c) cross-correlation values between the template images of IR and WV EBBTs for respective upper and middle height level AMVs (QI >0.85). As seen in Figure 2 (c), lower-height-level clouds (cumulus and so on) show smaller values of cross-correlation between IR and WV EBBTs. Xu et al. (1998) indicated that lower-height-level cloud can be distinguished by using the cross-correlation threshold of approximately 0.3. In this study, cloud targets below 400-hPa height-level from L1 with the cross-correlation less than 0.35 are assigned to 'stable-layer-base' which is computed by using IR EBBT of cloud pixels around the cloud top. Moreover, 1.5 % coldest pixels of the template image, which are sometimes corresponding to convective clouds in cyclones, are not used in calculation of L1. The application of procedure is arbitrary. Here, the threshold of 1.5 % was determined not to have significant influence on AMV heights. Under the use of all these schemes, the heights of "TEST AMVs" are finally obtained as shown in Figure 2 (d). The TEST AMVs are evaluated in the following section.

3.2 QUALITY OF TEST AMVS

(a) Quality to JMA's NWP first-guess field

This paragraph shows the characteristics of TEST AMVs in terms of quality against JMA's NWP (60 km Global Spectral Model (GSM)) first-guess. HA by using coldest pixel radiances within template image is the most common. Hence, first of all, AMVs computed by using TEST scheme described in section 3.1 are compared to AMVs which are assigned to the heights computed from the average of coldest pixel radiances. In below discussions, 6-hourly AMVs are investigated, which are computed by using three successive MTSAT-1R images at 15 minute intervals.

Figure 3 shows wind speed bias (BIAS; AMV minus JMA's NWP first-guess) of three kinds of AMVs which are assigned to heights computed by using various rate (10%, 15% and 25%) average of coldest pixel radiances within template image, and TEST AMVs at each height-level for one case.

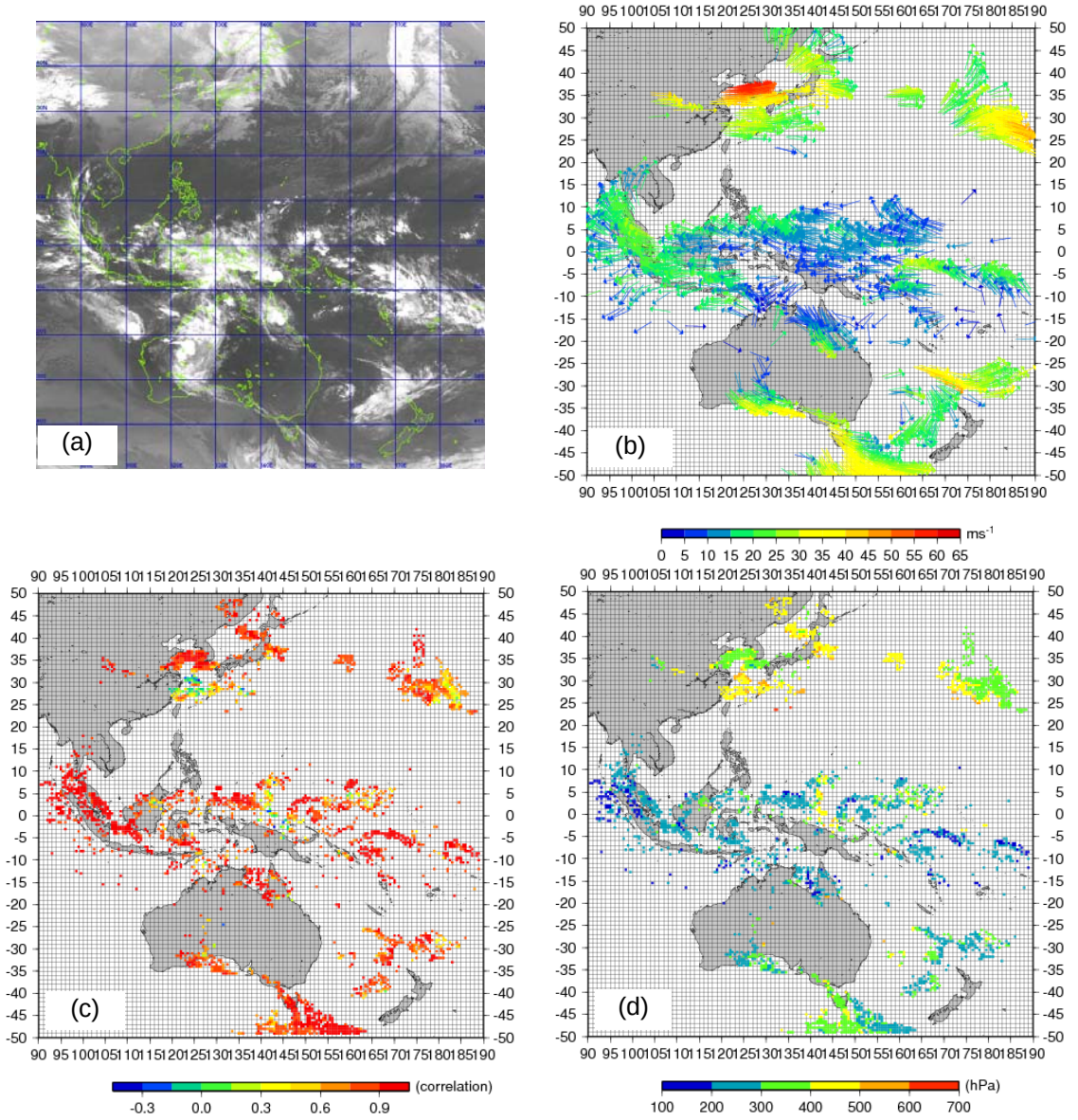

***Figure 2*: (a) IR EBBT image of MTSAT-1R, (b) wind vectors of AMVs (QI (with forecast check)>0.85), (c) cross-correlation values between the template images of IR and WV EBBT for respective AMVs (QI>0.85), and (d) heights of TEST AMVs (QI (with forecast check)>0.85) at 12 UTC on 10 March 2007.**

Figure 3 (a) shows that the use of coldest 10% average gives large slow BIASes at height-levels above 500 hPa for Northern and Southern Hemispheres and Tropics, because the heights are much higher than the best-fit level where the AMV and NWP wind match the best. Moreover, Figure 3 (b) shows that the use of coldest 15% average remains the large slow BIASes for Southern Hemisphere although they are mitigated compared to the use of coldest 10 % average. As seen in Figure 3 (c), the use of coldest 25 % average gives a better result than those of 10 and 15 % averages, however, large fast BIAS between 500 hPa and 600 hPa are recognized over Northern Hemisphere. In contrast, the BIASes of TEST AMVs are very small at respective height-levels for all the regions although the slow BIASes of approximately -3.0 m/s are recognized at height-levels between 300 hPa to 500 hPa for Southern Hemisphere.

Then, the qualities of current JMA's AMVs (hereafter called "RTN AMVs") and TEST AMVs are compared. Figure 4 (a) and (b) show the spatial distributions of vector difference (VD) against JMA's NWP first-guess for RTN AMVs and TEST AMVs (QI>0.85) for one case. In the comparison between Figure 4 (a) and (b), it is noticed that the coverage of TEST AMV data is larger than that of RTN AMVs, particularly, over the oceans in Southern Hemisphere and the Yellow Sea east to China (inside red circles). The magnitudes of VD are almost same for RTN AMVs and TEST AMVs over the all region. However, a few RTN AMVs over the Pacific Ocean have large VD beyond +45 m/s. Figure 4 (c) and (d) show the same as Figure 4 (a) and (b) respectively, but for BIAS. The magnitude of BIASes is nearly same between RTN AMVs and TEST AMVs for all the regions.

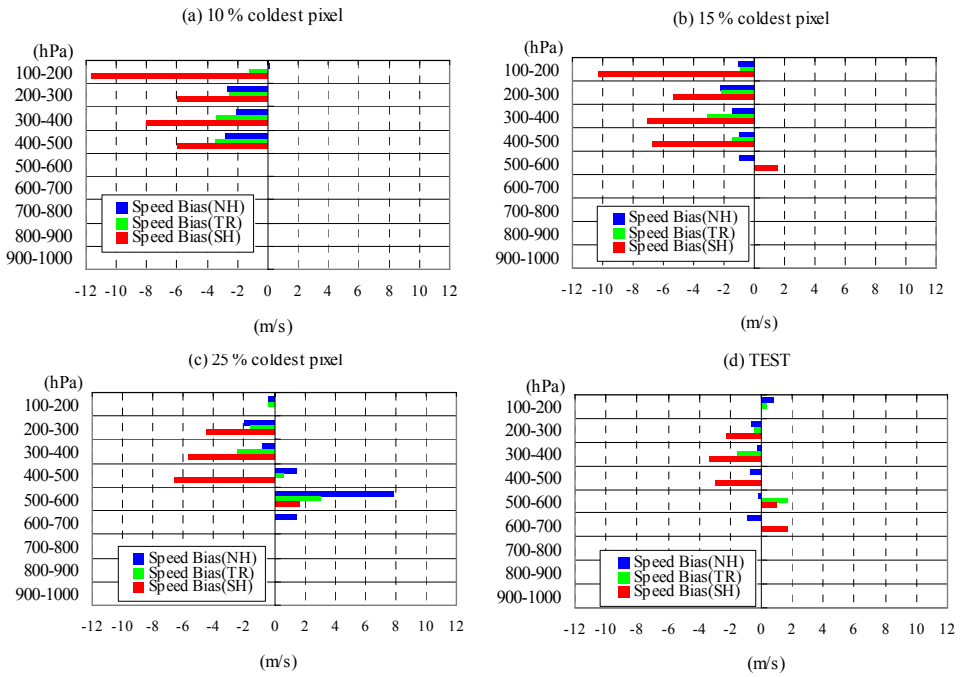

***Figure 3*: BIASes (AMV minus JMA's NWP (60km GSM) first-guess) of four AMVs, that is, AMVs assigned to heights computed from (a) 10 %, (b) 15 % and (c) 25% coldest-pixel-average radiances, and (d) TEST AMVs, respectively at each height level. NH, TR and SH mean Northern Hemisphere (between 20 N and 50 N), Tropics (between 20S and 20 N) and Southern Hemisphere (between 50S and 20S), respectively. The AMV data is for 00UTC 05 September 2007.**

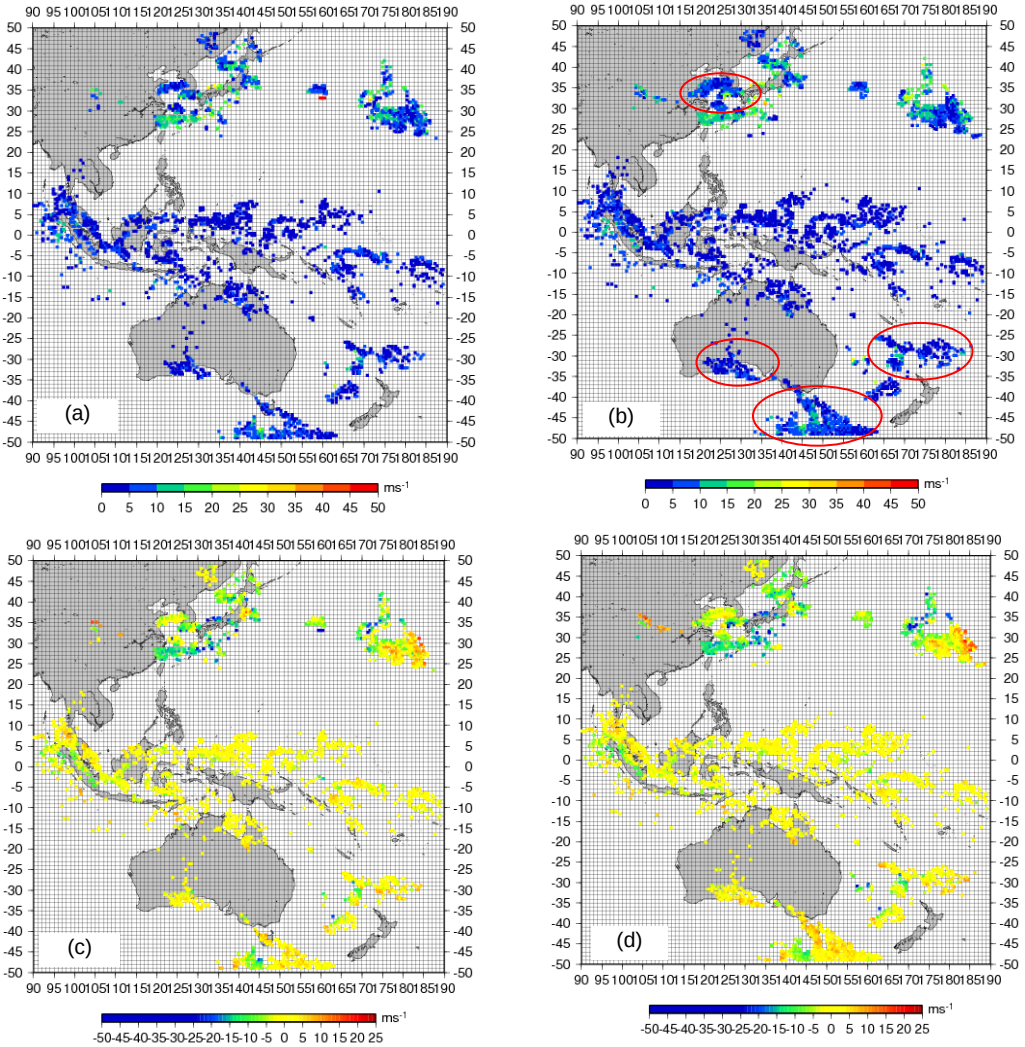

***Figure 4*: Vector Differences (VDs) of (a) RTN AMVs and (b) TEST AMVs, and BIASes of (c) RTN AMVs and (d) TEST AMVs against JMA's NWP (60km GSM) first-guess at 12 UTC on 10 March 2007.**

Figure 5 shows (a) BIASes and (b) numbers of RTN AMVs (Left) and TEST AMVs (Right) (QI>0.85) against JMA's NWP first-guess at each height level for March 2007. The number of TEST AMVs is larger than that of RTN AMVs, particularly above 500 hPa height-level. A fast BIAS between 600 and 700 hPa is observed in the statistics of RTN AMVs, and not observed for TEST AMVs. TEST scheme improves HA for some AMVs which are erroneously assigned to heights below 400 hPa height-level by RTN scheme. As the results, the fast BIASes between 600 and 700 hPa observed in RTN AMVs are reduced.

Figure 6 is the same as Figure 5, but for September 2007. In the comparison between Figure 6 (a) and (b), it is recognized that the fast BIAS of TEST AMVs at levels of 500 to 700 hPa is less than that of RTN AMVs. The monthly number of TEST AMVs is larger than that of RTN AMVs. These characteristics to JMA's NWP first-guess field are similar to those recognized in March 2007.

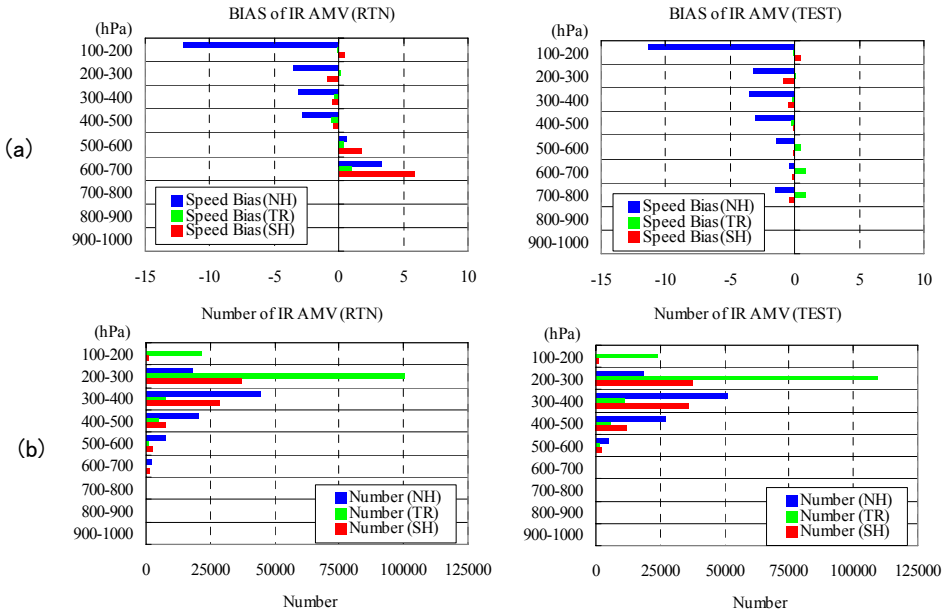

***Figure 5*: (a) BIAS (AMV minus JMA's NWP first guess) and (b) number of RTN (Left) and Test (Right) IR AMVs at each height level. NH, TR and SH mean Northern hemisphere (between 20 N and 50 N), Tropics (between 20S and 20 N) and Southern hemisphere (between 50S and 20S), respectively. The statistical month is March 2007.**

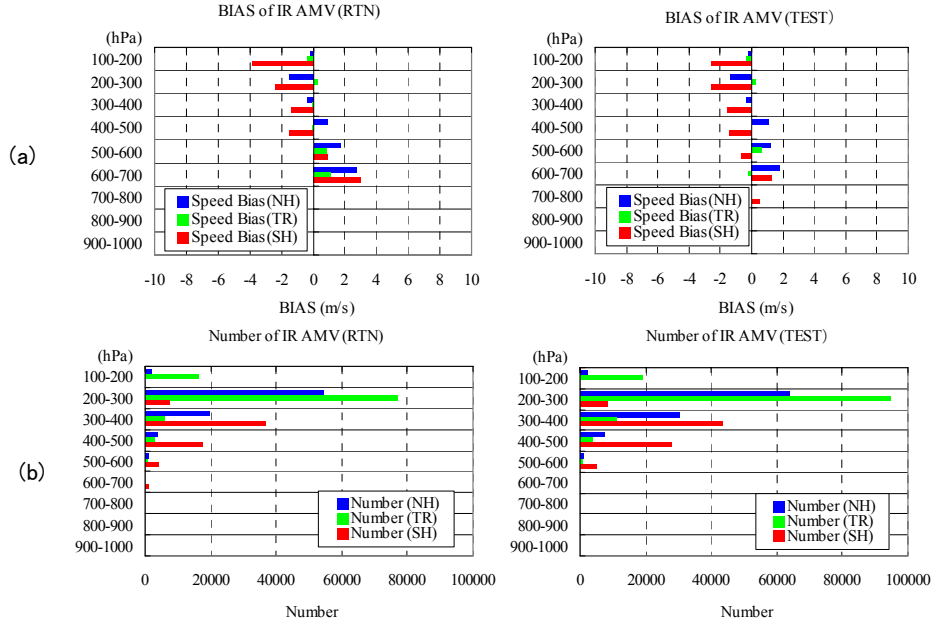

***Figure 6*: Same as Figure 5, but for September 2007.**

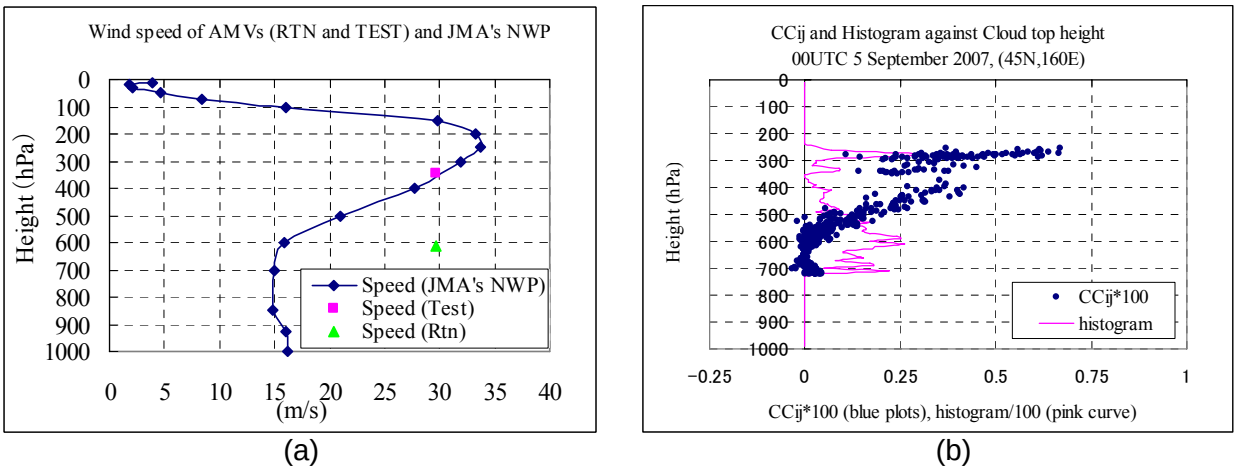

***Figure 7*: A case for RTN AMV and TEST AMV at a location (45N, 160E) at 00UTC 5 September 2007. (a) Wind speeds of AMVs (RTN AMVs (green plot) and TEST AMVs (Pink plot)) and interpolated JMA's NWP first-guess field (Blue curve), (b)individual-pixel CCij (Blue plots) against cloud-top height, and histogram of height (Pink curve).**

Figure 7 illustrates how these positive impacts are obtained for a typical case. Figure 7 (a) shows the wind speeds of RTN AMV and TEST AMV, and interpolated JMA's NWP first-guess at a location. The fast wind speed bias against JMA's NWP is observed for RTN AMV, but not found for TEST AMV. In Figure 7 (b), it is recognized that the enormous proportion of pixels within template image exist at height-levels between 500 and 600 hPa, while the maximum peak of CCij exists at around 300 hPa height-level. These situations explain that the improvement of fast speed bias at middle-height-level by introducing TEST scheme is due to the use of CCij.

(b) Quality to sonde observation winds

In the following, the performances of TEST AMVs to RTN AMVs are compared with reference to sonde observation.

Table 1 shows the monthly statistics of RTN AMVs and TEST AMVs (QI>0.85) against sonde observation winds for March 2007. At upper-height-level (above 400 hPa), the BIASes and RMSVDs of TEST AMVs are nearly same as those of RTN AMVs, and the numbers of TEST AMVs are 10 % larger or more than those of RTN AMVs for Northern and Southern Hemispheres and Tropics, respectively. At middle-height-level (700 hPa to 400 hPa), the slow BIAS of TEST AMVs is slightly larger than that of RTN AMVs for Northern Hemisphere although the RMSVD of TEST AMVs is nearly same as that of RTN AMVs. Over Tropics, both RMSVD and BIAS of TEST AMVs are better than those of RTN AMVs.

Table 2 is the same table as Table 1 but for September 2007. The slow BIAS of TEST AMVs at upper-height-level is slightly larger than that of RTN AMVs for Northern and Southern Hemispheres, while RMSVD is nearly same between RTN AMVs and TEST AMVs. At middle-height-level, the BIASes and RMSVDs are almost same between RTN AMVs and TEST AMVs.

Upper height level	NH (20N-50N)		TR (20S-20N)		SH (50S-20S)	
(Above 400 hPa)	RTN	TEST	RTN	TEST	RTN	TEST
MEAN SPEED (m/s)	33.4	33.4	14.5	14.5	23.4	23.1
BIAS (m/s)	-3.0	-3.1	-0.6	-0.8	-0.3	-0.6
RMSVD (m/s)	9.1	8.9	5.9	5.8	6.7	7.0
Number of collocated AMVs	6297	7084	7339	7955	2194	2373
Number of AMVs	31621	35197	59898	67311	34106	38013
Middle height level	NH (20N-50N)		TR (20S-20N)		SH (50S-20S)	
(700 hPa to 400 hPa)	RTN	TEST	RTN	TEST	RTN	TEST
MEAN SPEED (m/s)	25.7	25.2	11.1	11.1	16.1	17.2
BIAS (m/s)	-2.2	-3.8	-2.1	-1.4	-0.1	0.3
RMSVD (m/s)	9.0	9.3	5.3	4.7	5.4	5.7
Number of collocated AMVs	3365	3388	212	209	242	314
Number of AMVs	15562	16538	3098	3406	5945	7391

***Table 1*: Monthly statistics (MEAN SPEED, BIAS, RMSVD and NUMBER) of RTN AMVs and TEST AMVs (QI>0.85) against sonde observation. The statistical month is March 2007.**

Upper height level	NH (20N-50N)		TR (20S-20N)		SH (50S-20S)	
(Above 400 hPa)	RTN	TEST	RTN	TEST	RTN	TEST
MEAN SPEED (m/s)	24.9	24.5	14.9	14.8	28.5	29.0
BIAS (m/s)	-1.8	-2.1	-0.4	-0.7	-1.8	-2.6
RMSVD (m/s)	7.5	7.6	6.1	6.1	8.8	9.0
Number of collocated AMVs	9621	11883	4078	4896	832	951
Number of AMVs	37216	46912	45969	57298	20685	24117
Middle height level	NH (20N-50N)		TR (20S-20N)		SH (50S-20S)	
(700 hPa to 400 hPa)	RTN	TEST	RTN	TEST	RTN	TEST
MEAN SPEED (m/s)	18.2	18.4	10.4	9.9	23.5	22.4
BIAS (m/s)	-0.1	0.0	0.2	0.2	-2.4	-2.6
RMSVD (m/s)	5.7	5.9	4.3	4.3	8.0	8.4
Number of collocated AMVs	1018	1336	168	219	426	691
Number of AMVs	2586	4366	1879	2206	10875	15661

***Table 2*: Same as Table 3, but for September 2007.**

4 CONCLUDING REMARKS AND FUTURE PLAN

In this study, the effectiveness of contribution-rate to feature-tracking (CCij) on AMV height assignment is investigated. The weighted IR radiance (L1) of pixels within template image, balanced by CCij, is introduced to upper and middle height-level cloudy targets together with a scheme that identifies the cloud-type of AMV targets. In the TEST AMVs, the some positive impacts of CCij on the quality of AMVs are found.

The characteristics of TEST AMVs against AMVs assigned to heights computed from 10, 15 and 25 % coldest-pixel radiance average within template image are investigated for one case. The results show that large slow BIASes at height-levels above 500 hPa, which are observed in the AMVs assigned to heights from coldest-pixel radiance average, are improved in TEST AMVs, particularly, in winter hemisphere. Moreover, the fast BIASes of AMVs assigned to heights from 25 % coldest-pixel radiance average, which are observed at levels between 500 and 600 hPa, are improved by TEST scheme.

From the comparison between current JMA's AMVs (RTN) and TEST AMVs, two noticeable improvements of TEST AMVs to RTN AMVs are recognized, that is, the reduction of fast BIASes against JMA's NWP first-guess below 500 hPa and the increase of high-quality (QI>0.85) AMVs particularly at upper troposphere. Meanwhile, it is found that the slow BIASes of TEST AMVs are slightly larger than those of RTN AMVs in winter hemispheres. The increase of slow BIAS is probably because colder pixels tend to have larger CCij.

In the near future, after evaluations of more long-term monthly statistics against sonde observation and JMA's NWP first-guess, JMA plans to introduce TEST AMVs in operation. And JMA will continue to make efforts to reduce slow BIAS observed at upper troposphere in winter hemisphere from now on. In fact, the existence of slow BIAS over the middle latitudes is not only related to height assignment but also to the weakness of feature-tracking, for example, due to the strong jet stream with large curvature caused by extra-tropical cyclone. The change of template size is maybe one of the ways that can be used to mitigate the weakness of tracking.

In this study, it is confirmed that CCij is useful information for selecting contributive cloud pixels to appropriate decision of AMV heights. The information can be introduced in height assignment in various ways, using the weighted IR radiance of pixels or in conjunction with other products, for example, Cloud Analysis product (Borde and Oyama, 2008).

REFERENCES

ASD; 'MSG Meteorological Products Extraction Facility Algorithm Specification Document' edited by EUMETSAT. Reference: EUM.MSG.SPE.022.

Borde, R. ,2006: AMV height assignment methods with Meteosat-8, Proceedings of 8th International Winds Workshop.

Borde, R. and R. Oyama, 2008: A direct link between feature tracking and height assignment of operational AMVs, Proceedings of 9th International Winds Workshop.

Büche, G., et al., 2006: Water vapor structure displacements from cloud-free METEOSAT scenes and their interpretation for the wind field, J. Appl. Meteor., 45, 556-575.

Daniels, J., et al., 2002: Status and development of GOES wind products at NOAA/NESDIS, Proceedings of 6th International Winds Workshop, EUMETSAT, 71-80.

Le Marshall, J., N .Pescod, A. Khaw, and G. Allan 19, 1993: The real-time generation and application of cloud-drift winds in the Australian region. Aust. Meteor. Mag., 42, ((3),) 89-103.

Nieman, N. J., Schmetz and W.P. Menzel, 1993: A comparison of several techniques to assign heights to cloud tracers, J. Appl. Meteorol., 32, 1559-1568.

Oyama, R. and K. Shimoji, 2008: Status of and future plans for JMA's Atmospheric motion vectors, Proceedings of 9th International Winds Workshop.

Schmetz, J., K. Holmlund, J. Hoffman, B. Strauss, B. Mason, V. Gartner, A. Koch, and L. van de Berg, 1993, Operational cloud-motion winds from Meteosat infrared images. *J. Appl. Meteor.,* **32,** 1206–1225.

Xu, J., Q. Zhang, F. Xiang, L. Jian, 1998: Cloud motion winds from FY-2 and GMS-5 meteorological satellites, Proceedings of 4th International Winds Workshop, 41-48.